Systematic Analysis of Convection for OTREC and PREDICT

Ž. Fuchs-Stone[1,2], S. Sentić[1], D. J. Raymond[1,2], and P. Bechtold[3]

[1]Climate and Water Consotrium, New Mexico Tech, 801 Leroy Place, Socorro, NM.

[2]Physics Department, New Mexico Tech, 801 Leroy Place, Socorro, NM.

[3]European Centre for Medium-Range Weather Forecasts, Shinfield Park, Reading, United Kingdom

Corresponding author: Željka Fuchs-Stone (zeljka.fuchs@nmt.edu)

Key points:

- Both boundary layer (DCIN) and free troposphere (saturation fraction and instability index) are very important for development of convection.
- Strong convection correlates with saturation fraction and anti-correlates with instability index and DCIN in a similar manner regardless of the environment.
- Weak and null convection shows a variety of behavior in different environments.

Abstract

The systematic analysis of convection and the environment is performed for two field projects, OTREC and PREDICT by implementing 3DVAR on drospondes data sets.

Vertically integrated moisture convergence is taken to be a proxy for convection. The interplay between the thermodynamic parameters is examined for three different stages of convection: strong convection, medium to weak and weak to null convection. It is found that for strong convection saturation fraction anti-correlates with instability index and DCIN in a similar manner for all analyzed regions of PREDICT and OTREC, while the differences in the environment become more pronounced as we move towards weak and null convection.

ECMWF operational model is used to look at the time evolution of convection. As convection increases, saturation fraction increases while instability index and DCIN decrease.

The boundary layer and free troposphere both play an important role in convection development in OTREC and PREDICT regions.

Plain Language Summary

Convection in the tropics is the main mechanism that brings bad weather, storms and hurricanes. Understanding how convection develops and what it depends on is a question that we have been trying to answer for many decades. The characteristics of the environment can help in this task. The data from two field projects, OTREC2019 and PREDICT2010 are analyzed here to show what characteristics of the environment we should pay attention to. This can help us in improving the weather models and forecast.

1. Introduction

Mesoscale convective systems (MCS) are responsible for most rain in the tropics, Houze (1989). They are ensembles of convection that one can regard as entraining plumes of 1 - 5 km diameter that go through their life cycle almost independently of one another. If the convection grows in time that implies that the number of plumes is getting larger and the area of convection covers a larger area, while when convection decays, their number is getting smaller. This school of thought studies the evolution, i.e. growth and decay of MCSs as well as their detailed structure (Arakawa and Shubert 1974; Zipser, 1969, 1977; Houze, 1989, 2004; etc.; personal communication with Ed Zipser).

Another school of thought tries to study the broader properties of MCSs and most importantly their interaction with the environment, Raymond et al. (2011). This approach does not look at the individual structure of the MCSs, but how the environment governs their overall characteristics. The goal is to identify the thermodynamic properties of the environment that lead to MCSs. If one gets those right, it would be possible to correctly parametrize convection, Raymond and Fuchs-Stone (2020).

What properties of the environment guide convection? Is it the boundary layer, free troposphere or both? There are many papers that suggest that the boundary layer is responsible for the

intertropical convergence zone, ITCZ (Riehl et al., 1951; Lindzen and Nigam, 1987; Battisti et al., 1999; Tomas et al., 1999; Stevens et al., 2002). Back and Bretherton (2009) postulate two types of convection, one that is generated by the boundary layer convergence and another that is generated by free troposphere noting that the boundary layer convergence is of more importance in east and central Pacific ITCZ. Raymond (2017) advocates for the importance of thermodynamic factors mainly in the free troposphere.

In this paper, we aim to systematically look at the data from the field projects OTREC and PREDICT as together they provide a data set for a wide range of sea surface temperatures (SST), 298 to 304 K, in the tropics. Figure 1 shows the OTREC flight locations and SST, while Figure 2 shows the same for PREDICT.

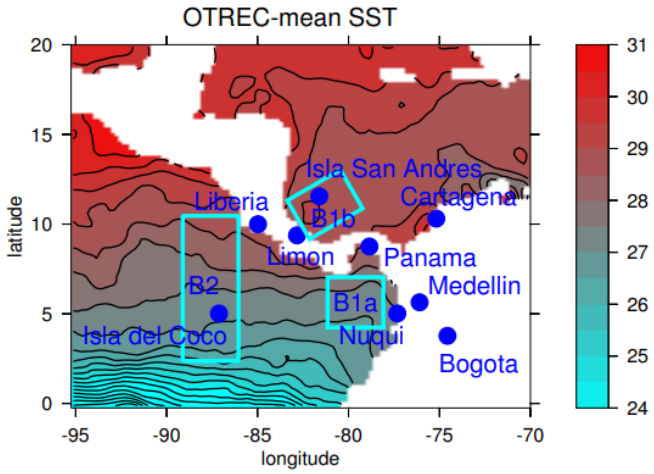

Figure 1: OTREC flight area given by blue boxes and NOAA AVHRR SST averaged over the project period (Raymond and Fuchs, 2020).

OTREC2019 (Organization of Tropical East Pacific Convection), Fuchs-Stone et al. (2020), studied all phases of convection over the East Pacific and Southwest Caribbean from Liberia, Costa Rica using the NSF/NCAR Gulfstream V aircraft. 22 research missions were flown and 648 dropsondes were successfully deployed in a grid for flight boxes B1a, the Colombian box; B1b, the Caribbean box; and B2, the Eastern Pacific ITCZ box.

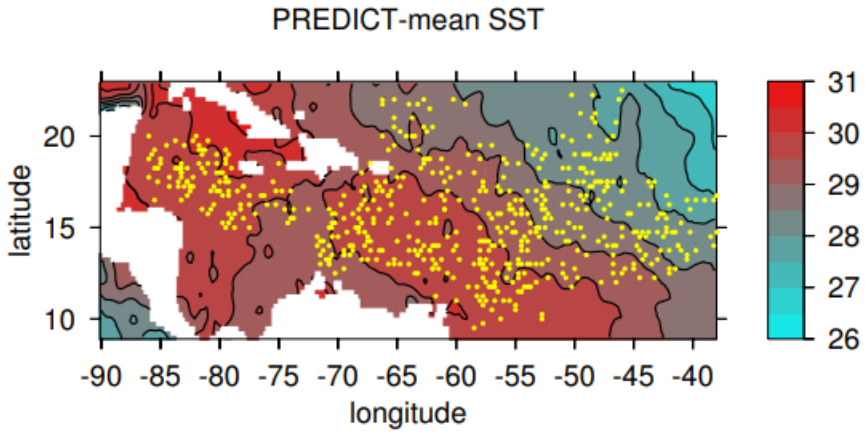

Figure 2: Flight area and SST (NOAA AVHRR) during PREDICT. Yellow dots are representative of locations where dropsondes were deployed (Raymond and Fuchs, 2020).

PREDICT2010 (Pre-Depression Investigation of Cloud-Systems in the Tropics), Montgomery et al. (2012), studied systems with potential to develop into tropical cyclones in the Western Atlantic and Caribbean using the NSF/NCAR Gulfstream V aircraft. 26 research missions were flown and 547 drospondes were deployed.

Our results are based primarily on dropsonde data on which three-dimensional variational analysis (3DVAR) is performed to obtain regular grids of data 0.25 by 0.25 degree (Lopez and Raymond, 2011; Raymond and Lopez, 2011; Raymond et al., 2011; Montgomery et al., 2012; Gjorgjievska and Raymond, 2014; Juracic and Raymond, 2016; Fuchs-Stone et al., 2020; Raymond and Fuchs-Stone, 2020). The data set for dropsondes used in this paper is NCAR/EOL AVAPS Dropsonde Quality Controlled Data Version 1.0, Voemel, H. (2019).

Section 2 defines the thermodynamic parameters used to analyze convection from OTREC and PREDICT, section 3 presents the results and their interpretation, while conclusions are given in section 4.

2. Thermodynamic parameters

The chosen proxy for convection is vertically integrated moisture convergence that is defined as:

$$\mathrm{MC} = -\int \nabla \cdot (\rho \boldsymbol{v} r)$$

where ρ is the density, $\boldsymbol{v}$ is the horizontal components of velocity and r is the mixing ratio.

The thermodynamic parameters shown to be of most importance (Raymond and Fuchs, 2020) that will be analyzed and compared to moisture convergence, i.e. convection, are saturation fraction, instability index and deep convective inhibition.

The saturation fraction is defined as precipitable water over the saturated precipitable water

$$SF = \frac{\int r dp}{\int r_s dp}$$

where r_s is the saturation mixing ratio and p is the pressure. It is a measure for column relative humidity.

The instability index is defined as:

$$II = s_{low} - s_{high}$$

where s_{low} is the saturated moist entropy averaged over the altitude ranges of 1-3 km while s_{high} is averaged over 5-7 km. The instability index is a measure of low to mid-tropospheric moist convective instability. Lower, but still positive, values are associated with higher saturation fraction and more rainfall (Raymond et al., 2014, Gjorgjievska and Raymond, 2014, Raymond et al., 2015, Sentic et al., 2015, Raymond and Flores, 2016, Singh et al., 2019, Raymond and Kilroy, 2019). Moisture quasi-equilibrium theory postulates that the instability index is inversely proportional to saturation fraction, Raymond et al. (2014).

Deep convective inhibition (DCIN) is defined as

$$DCIN = s_{th}^{*} - s_{bl}$$

where s_{th}^{*}, the threshold entropy, is the average of the saturated moist entropy in the 1.5 - 2 km layer and s_{bl} is the boundary layer moist entropy averaged over the 0 - 1 km layer.

We will also look at the difference between mass flux profiles defined as:

$$\Delta MF = mfluxhigh - mfluxlow$$

where $mfluxhigh$ is the vertical mass flux averaged over 7 – 9 km and $mfluxlow$ over 3 – 5 km. The vertical mass flux profile is defined as the horizontally averaged product of density and vertical speed *w*:

$$M(z) = \overline{\rho w}.$$

ΔMF is a measure of top-heaviness of convection, if it is positive the convection is more top heavy, while if it is negative it is more bottom heavy.

3. Results

3.1 Convection and thermodynamic parameters as a function of SST

To systematically analyze the dropsonde data from field projects OTREC and PREDICT at the wide range of SSTs, we first analyze how moisture convergence, a proxy for convection, the thermodynamic parameters and mass flux difference ΔMF relate to SST. Figure 3 thus shows moisture convergence, saturation fraction, instability index, DCIN and ΔMF as a function of SST. Each dot represents the average in a one by one degree box obtained from the 3DVAR. PREDICT

data is shown in green, the data for the Eastern Pacific ITCZ box B2 in blue, the Pacific box off the coast of Colombia, B1a, data is shown in red and the data for the Caribbean B1b box is shown in black. There is an overlap between PREDICT data, B1b data and north B2 data due to higher SSTs as well as between the south part of B2 and B1a at the lower SSTs.

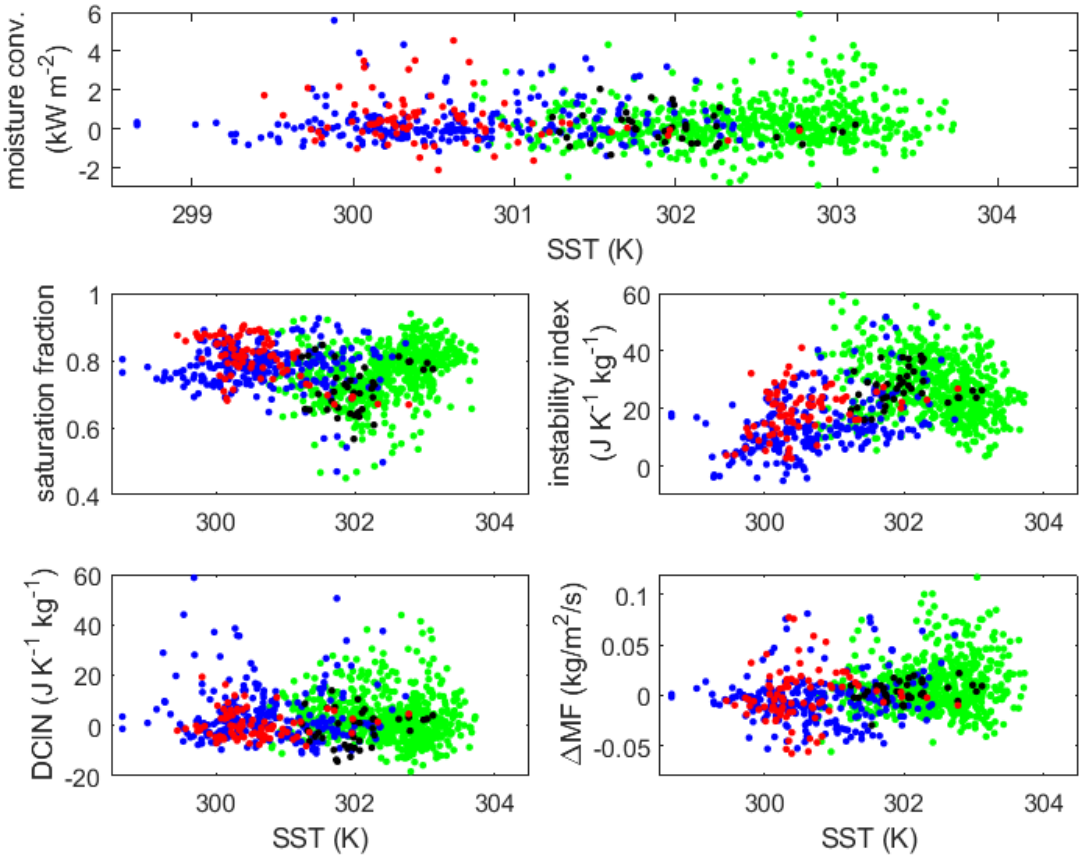

Figure 3: Dependence of moisture convergence, saturation fraction, instability index, DCIN and ΔMF on SST for OTREC and PREDICT. Green dots are PREDICT data, blue Eastern Pacific ITCZ, red Colombian box and black Caribbean box.

From Figure 3, we see that moisture convergence is independent of SST. Strong convection can occur at any values of shown SSTs except perhaps for its lowest values (299 K). This agrees with the fact that during OTREC, we observed only one convective event in the southern part of B2 box at 4 N latitude, Fuchs-Stone et al. (2020). It is interesting to note that although OTREC looked at all scenarios of convection including the null one, while PREDICT targeted tropical storm development, moisture convergence exhibits wide ranges of values in both data sets. In other words, both OTREC and PREDICT data show strong, medium, weak and null convection.

Looking at the saturation fraction dependence on SST, we see a uniform spread, i.e. there is no dependence of saturation fraction on SST except perhaps for PREDICT data that also shows lower

values of saturation fraction. This might be due to the particular nature of the PREDICT domain. Those lower values of saturation fraction are not associated with deep convection.

The instability index as shown in Figure 3 is clearly a function of SST with higher SSTs corresponding to larger values of the instability index. This comes as no surprise as the instability index is defined by using the saturated moist entropy, i.e. the temperature just above the boundary layer. Note that in the regions of large mid-level vorticity it is possible to have low instability index regardless of SST, Raymond et al. (2014).

DCIN appears to be independent of SST. Unlike the instability index and saturation fraction that mostly describe the free or full troposphere, DCIN describes the boundary layer. Low and negative DCIN mean that there is no inversion or inversion is weak and convection is free to develop. The high values of DCIN at the low values of SST seen by blue dots in Figure 3 show the area in south part of B2 with inversion.

Mass flux difference ΔMF, that is the measure for top-heaviness of convection, has higher and positive values for higher SSTs, while it is negative for lower SSTs. This implies that at lower SSTs we have prevailing bottom heavy convection, while for higher SSTs it is mostly top heavy. Similar result was obtained by Raymond and Fuchs (2020) shown in their Figure 11.

To summarize the findings from Figure 3, lower SST is associated with lower values of instability index and bottom heavy vertical mass flux profile while higher SST is associated with higher values of instability index and top heavy vertical mass flux profile. DCIN, saturation fraction and moisture convergence do not depend on SST.

3.2 The interplay between convection and thermodynamic parameters

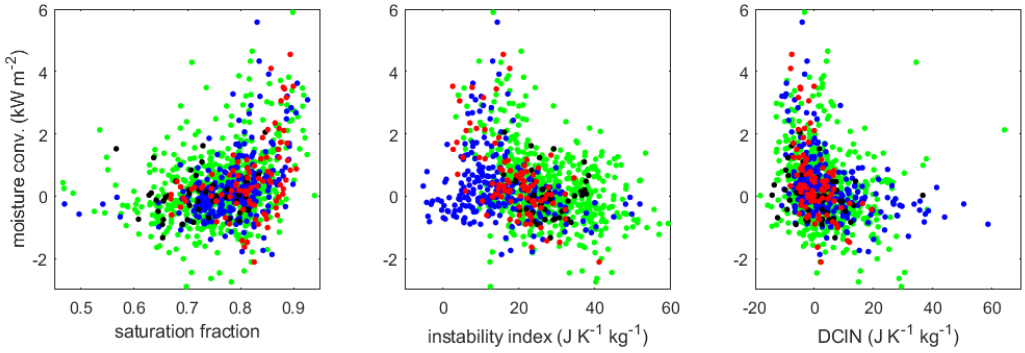

Figure 4: Scatter plot of moisture convergence and saturation fraction, instability index and DCIN. Green dots are PREDICT data, blue Eastern Pacific ITCZ, red Colombian box and black Caribbean box.

Figure 4 shows how our thermodynamic parameters saturation fraction, instability index and DCIN correlate with moisture convergence, i.e. convection. We see that higher values of saturation fraction lead to more convection. The opposite is true for the instability index where lower values

correspond to more convection. Similarly to the instability index, but perhaps even more pronounced, negative and small values of DCIN lead to more convection.

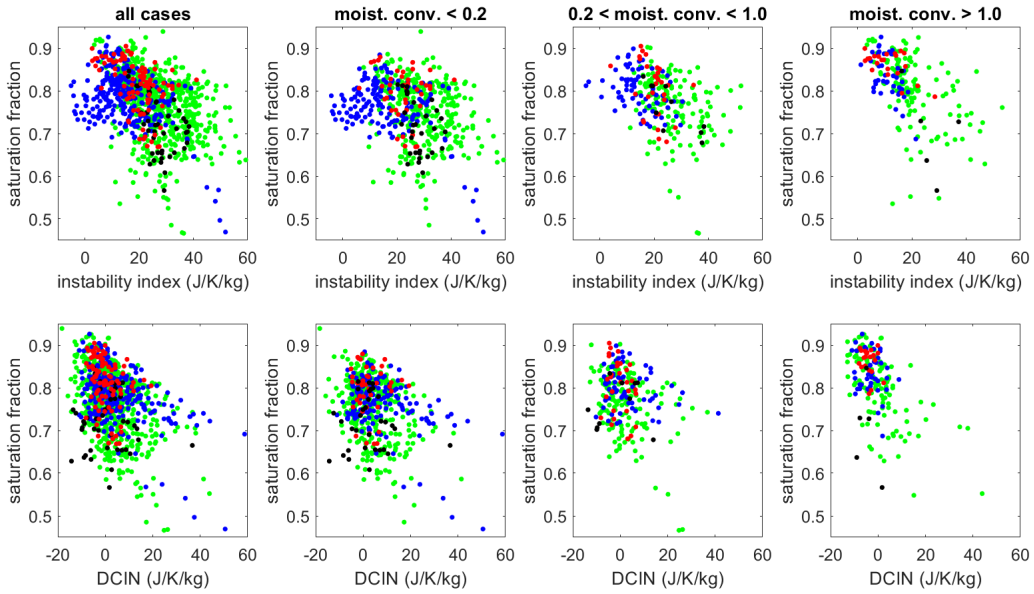

Figure 5: Scatter plots between saturation fraction and instability index (top panel) and saturation fraction and DCIN (bottom panel) for all cases, null to weak convection, weak to medium convection and strong convection.

To decipher Figure 4, that includes all cases from null to strong convection, we now set out to look at the relationships between our thermodynamic parameters saturation fraction, instability index and DCIN for different phases of convection. We define convection by the strength of vertically integrated moisture convergence. If moisture convergence is greater than 1 kWm^{-2} we define it as strong convection, if it is between 0.2 and 1 kWm^{-2} weak to medium convection and if it is less than 0.2 kWm^{-2} weak to null convection.

Figure 5 shows scatter plots between saturation fraction and instability index (top panel) and saturation fraction and DCIN (bottom panel) for, starting from the left in the figure, all cases, null to weak convection, weak to medium convection and strong convection cases. For strong convective cases the saturation fraction and instability index show a clear anti-correlation as per moisture quasi-equilibrium theory. The scatter plot between saturation fraction and DCIN shows without a doubt that negative or very small DCIN is required for strong convection. The scatter plot for weak to medium convection tells a similar story, but with more scattering. As expected the saturation fraction can be lower and instability index and DCIN higher. For weak to null convection, the scattering is even wider in both saturation fraction vs instability index and saturation fraction vs DCIN. This is to be expected as when there is weak or null convection the moisture quasi-equilibrium theory does not hold as the environment is too dry and DCIN naturally turns towards higher positive values. However, it is interesting to note some differences between the sets of data. The Eastern Pacific ITCZ box B2, even in weak to null cases, shows high

saturation fraction values and low instability index, while we don't see the same in other regions. The scattering is more pronounced for PREDICT and B2 data than for others.

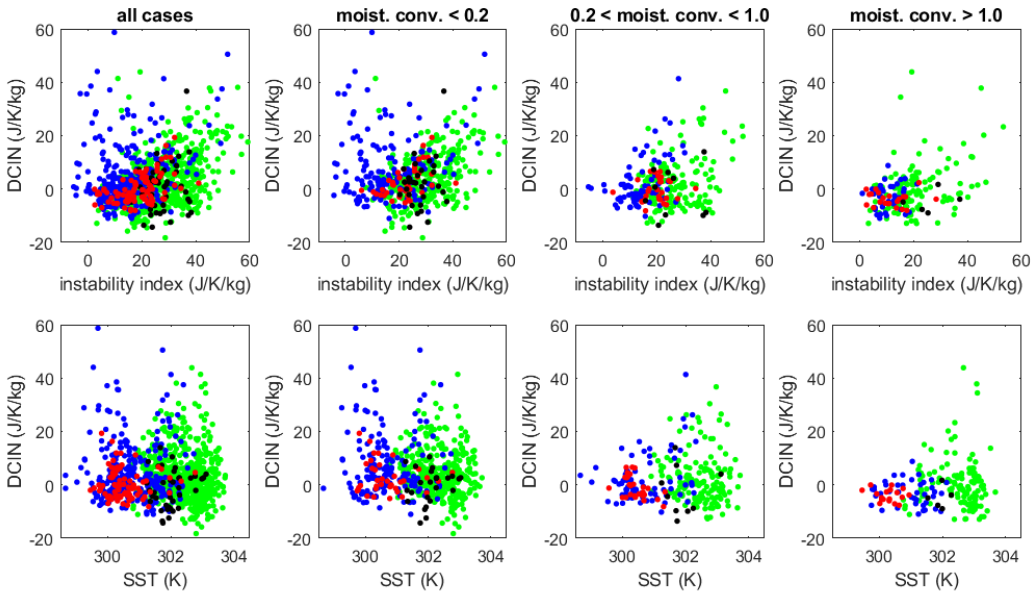

Figure 6: Scatter plots between DCIN and instability index (top panel) and DCIN and SST (bottom panel) for all cases, null to weak convection, weak to medium convection and strong convection.

Lastly, let's look at the relationship between DCIN and instability index and DCIN and SST for different phases of convection. Figure 6 shows the scatter plots between DCIN and instability index (top panel) and DCIN and SST (bottom panel). In a regime of strong convection, small DCIN corresponds to small instability index. Similar is true for weak to medium convection except that there is more scattering. In a regime of null to weak convection the scattering is even more pronounced with the possibility of high values of DCIN and low values of instability index in the B2 data. Looking at the bottom panel, we can see that those cases correspond to the ones at the southern part of the B2 box where inversion is present, also seen in EPIC2001 (East Pacific Investigation of Climate) data, Raymond (2017). For weak to medium convection as well as for strong convection, there is no dependence of DCIN on SST.

Figures 3 – 6 tell an interesting story. Strong convection seems to be similar in all regions, no matter what the SST is, whether we are close to land or not, once there is significant convection, there is no doubt that moisture convergence depends on high saturation fraction, low instability index and low DCIN. Furthermore, saturation fraction anti-correlates with instability index and DCIN in a similar manner. When convection is weak and the environment is dry, the time scale for convection to adjust the moisture to the equilibrium value for a given value of instability index is long and this anti-correlation is not necessarily observed. DCIN takes up higher values indicating inversion. The differences between observed regions are more apparent in the cases of null to weak convection and this is a subject for future research.

3.3 Vertical mass flux profiles

Differences in vertical mass flux profiles could indicate differences between convection in different regions. Figure 7 shows the average vertical mass flux profiles for strong convection when moisture convergence is greater than 1 kWm^{-2} for 3 OTREC regions as well as for PREDICT.

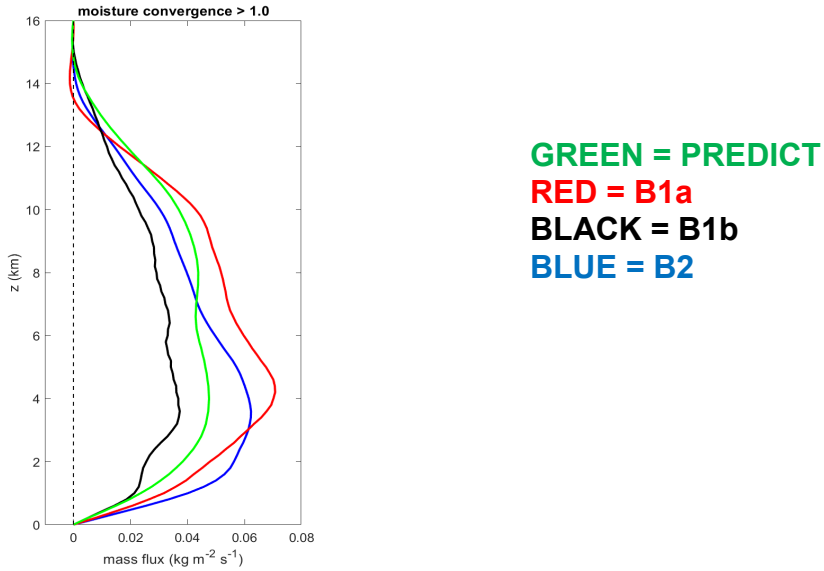

Figure 7: Averaged vertical mass flux profiles for PREDICT and OTREC for strong convection

From Figure 7 we can see that on average all vertical mass flux profiles in strong convection show deep vertical mass flux profiles. The profiles for PREDICT and the Caribbean B1b box are similar, with higher values in PREDICT. This might be because during OTREC we weren't able to fly into many strong convective cases in B1b, in fact, there were only 3 and they were not too strong, Fuchs-Stone et al. (2020). The vertical mass flux profiles for the Eastern Pacific ITCZ box B2 and the Colombian box B1a have even higher values than PREDICT and B1b. The mass flux profile in B1a box is more top-heavy than the one in B2 box.

3.4 Time evolution

To look at the time evolution of the convective cases, we first use the 3DVAR data from OTREC to define convective one by one degree box averages, defined as boxes with moisture convergence greater than 1 kWm^{-2}. We then average the European Centre for Medium-Range Weather Forecasts (ECMWF) operational model data in boxes with the same longitude and latitude for all times of the same day. Then we average all the hourly values. The same method is applied to the Geostationary Operational Environmental Satellite (GOES-16) brightness temperature. The results are shown in Figure 8.

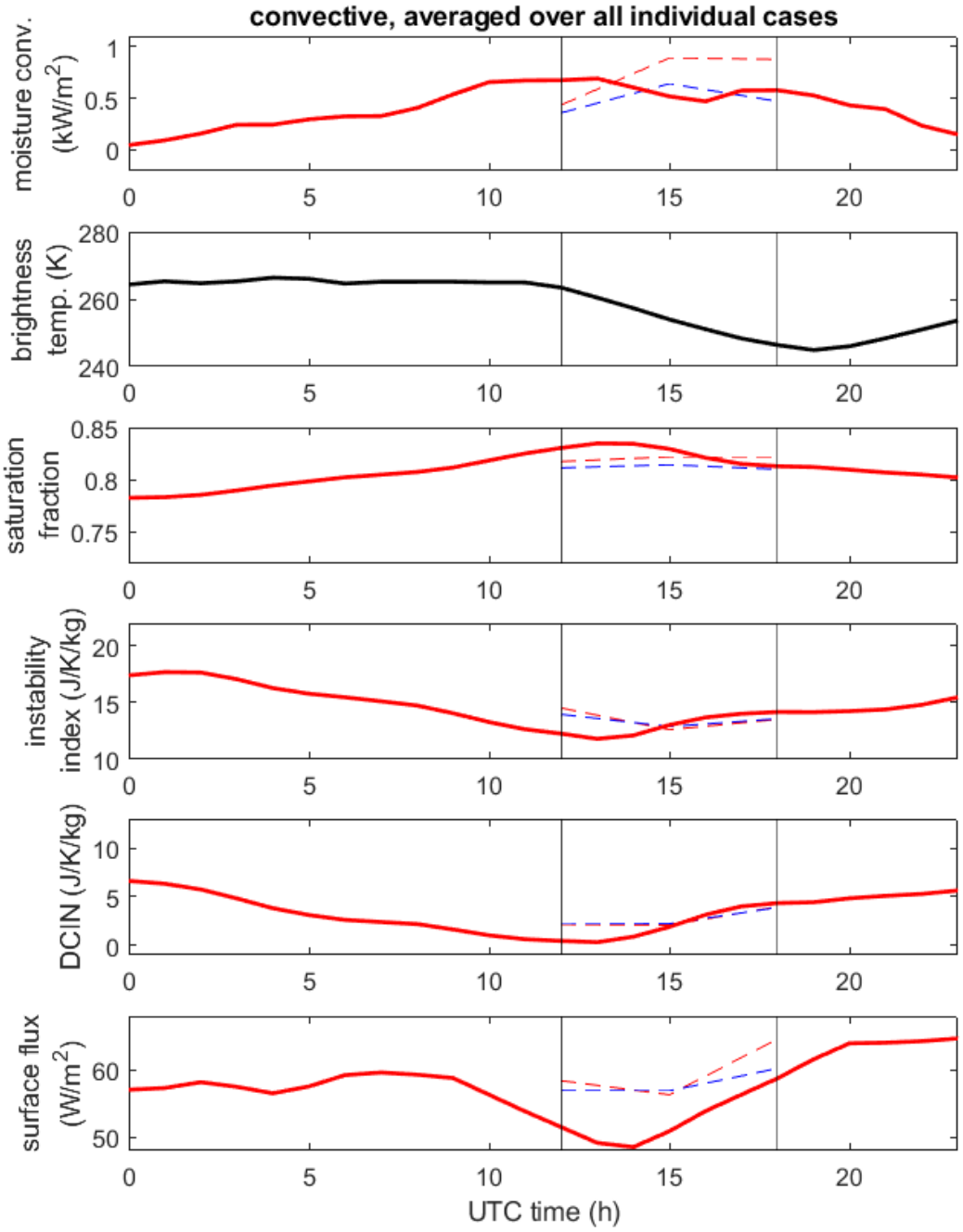

Figure 8: Moisture convergence, GOES-16 brightness temperature, saturation fraction, instability index, DCIN and surface latent heat fluxes averaged over all strong convective cases from OTREC. Solid red line represents ECMWF operational model results, solid black line GOES-16 results, while red and blue dashed lines show results from operational ECMWF model with and without dropsondes assimilated respectively.

Figure 8 shows moisture convergence, brightness temperature from the GOES-16, saturation fraction, instability index, DCIN and surface latent heat fluxes averaged over all strong convective cases from OTREC as a function of time. The vertical lines bound the time of a day when OTREC dropsondes were deployed and assimilated into the EC model (12 to 18 UTC). The red solid line shows the results from the ECMWF operational model.

We can see that the convection represented by moisture convergence peaks between 10 and 13 hours UTC, 4 to 7 am local time. This agrees with our observations while in the field. On average convection was developing in the very early morning hours, becoming stratiform around 10 am local time, 16 UTC. The black solid line in the second panel represents the brightness temperature from satellite observations GOES-16 for the same convective cases. Its minimum lags the maximum of the moisture convergence from the EC model due to the lag between convection and resulting stratiform cloudiness as the upper troposphere needs time to become optically thick, Bechtold et al. (2014). This gives us confidence in EC model of moisture convergence evolution as of the other parameters.

The red and the blue dashed lines represent the results from the EC operational model ran for 6 hours when our research flights took place. The intention is to compare the model with and without dropsondes to gain more confidence in the results of the model outside of that timeline. The run in which dropsonde data were assimilated is shown in red dashed line, while the one without the dropsondes assimilated is shown in blue dashed line. We can see that the model does very well when it calculates saturation fraction, instability index, DCIN and to some degree surface fluxes regardless to dropsondes being assimilated. The biggest difference is seen in the moisture convergence. The model underestimates moisture convergence when the dropsondes are not assimilated. This is why we looked at the GOES-16 brightness temperature as well.

We now look at the time evolution for moisture convergence, saturation fraction, instability index, DCIN and surface latent heat fluxes (Yu and Weller, 2008), from the EC model represented by red solid line. Prior to the peak in the moisture convergence saturation fraction increases while the instability index and DCIN decrease. They reach their maximum (saturation fraction) and minima (instability index and DCIN) at the same time, a bit after the maximum in moisture convergence. The reason behind this lag might be that sacrificial convection seen by moisture convergence has to first moisten the environment as per moisture quasi-equilibrium theory. The surface latent heat fluxes, Yu and Weller (2008), shown in bottom panel of Figure 8 decrease prior to convection due to a decrease in the surface wind speed.

4. Conclusions

The goal of this study is to systematically look at the 3DVAR analysis from the drosponde data for the field projects OTREC and PREDICT to see how convection behaves in different environments and if the convection is different depending on its strength. Some of the questions that we try to answer are: Does convection change with different SSTs and is it different if there is proximity to land? Is convection different if it is strong, medium or weak in different environments? OTREC data covers 3 diverse environments. The research flight area in the Eastern Pacific ITCZ, B2, covers the region with strong meridional sea surface temperature gradients,

while B1b, the Caribbean region, covers the area with uniform and high SSTs. B1a box just off the coast of Colombia covers the environment of lower SSTs in the proximity of land. The PREDICT data covers a vast region of the western Atlantic and Caribbean, a region with high SSTs and higher latitudes than OTREC.

We take vertically integrated moisture convergence as a proxy for convection. The thermodynamic parameters used to describe convection are saturation fraction, instability index and DCIN. We first look at the dependence of convection, thermodynamic parameters and mass flux difference on SST to get a general picture. We see that deep convection can occur at any observed SST higher than 299.5 K which corresponds to well-known 26.5 C threshold for development of tropical disturbances and deep convection, Palmen (1948) and Grey (1968). Convection, saturation fraction and DCIN do not depend on SST, while instability index and mass flux difference do. Lower SST regions have smaller instability index and more bottom heavy vertical mass flux while higher SST regions have larger instability index and more top heavy convection.

Classifying convection into strong, medium, and weak to null and looking at the interplay of convection and thermodynamic parameters within those limits tells an interesting story. Strong convection looks very similar regardless to the environment, SST, proximity to land, different latitude etc. Moisture convergence, i.e. convection is strongly correlated with saturation fraction and anti-correlated with instability index and DCIN. Furthermore, saturation fraction shows similar anti-correlation with instability index and DCIN for every region that we have looked at. This implies that both, the boundary layer (DCIN) and free troposphere (saturation fraction and instability index) are very important for development of convection.

As we move towards medium and weak to null convection, the story becomes more complicated. The above correlations are less pronounced and more scattered. When there is no convection or convection is very weak, the environment looks different depending on the area we look at and those regional differences are left for future research.

The time evolution of moisture convergence, thermodynamic parameters and surface fluxes is analyzed using the ECMWF operational model for the events with strong convection during OTREC. Before the peak of convection saturation fraction increases and instability index and DCIN decrease. Maxima and minima of saturation fraction, instability index and DCIN are reached simultaneously. The surface latent heat fluxes decrease prior to convection. The significance of the impact of surface fluxes is not certain and is left for future research.

It is important to note that we are looking at convection and the environment rather than the evolution of individual plumes. Such analysis gives broad statistical answers and could help improve cumulus parametrizations, Raymond and Fuchs-Stone (2020).

Acknowledgments

We would like to acknowledge operational, technical and scientific support provided by NCAR's Earth Observing Laboratory, sponsored by the National Science Foundation. The NCAR/EOL AVAPS Dropsonde QC Data DOI: https://doi.org/10.26023/EHRT-TN96-9W04. Data is provided by NCAR/EOL under the sponsorship of the National Science Foundation https://data.eol.ucar.edu/. We thank students Katie Jensen and Marc Gross for their work on GOES-16 data. This work was supported by National Science Foundation grant 1758513.

References

Arakawa, A. and W. H. Schubert, (1974), Interaction of a cumulus cloud ensemble with the large-scale environment, Part I. *J. Atmos. Sci.*, 31, 674-701.

Back, L. E., and C. S. Bretherton, (2009), On the relationship between SST gradients, boundary layer winds, and convergence over the tropical oceans, *J. Climate*, 33, 4182-4196.

Battisti, D. S., E. S. Sarachik, and A. C. Hirst, (1999), A consistent model for the large-scale steady surface atmospheric circulation in the tropics, *J. Climate*, 12, 2956-2964.

Bechtold, P., N. Semane, P. Lopez, J. Chaboureau, A. Beljaars, and N. Bormann, 2014: Representing Equilibrium and Nonequilibrium Convection in Large-Scale Models. *J. Atmos. Sci.*, **71**, 734–753, https://doi.org/10.1175/JAS-D-13-0163.1.

Emanuel, K., 2020, Slow modes of the equatorial waveguide. *J. Atmos. Sci.*, **77**, 1575-1582, doi:10.1175/jas-d-19-0281.1.

Fuchs, Ž. and Raymond, D. J, (2017), A simple model of intraseasonal oscillations, *J. Adv. Model. Earth Syst.*, 9, 1195– 1211, doi:10.1002/2017MS000963.

Fuchs-Stone, Z., D. J. Raymond and S. Sentic, (2020), OTREC2019: Convection over the East Pacific and Southwest Caribbean. *Geophys. Res. Lett.*, 47, doi:10.1029/2020GL087564.

Gjorgjievska, S. and D. J. Raymond, (2014), Interaction between dynamics and thermodynamics during tropical cyclogenesis, *Atmos. Chem. Phys*., 14, 3065-3082.

Gray, W. M., (1968), Global view of the origin of tropical disturbances and storms, *Mon. Wea. Rev.*, **96**, 669–700,

https://doi.org/10.1175/1520-0493(1968)096<0669:GVOTOO>2.0.CO;2.

Houze, R. A., (1989), Observed structure of mesoscale convective systems and implications for large-scale heating. *Quart. J. Roy. Meteor. Soc.*, 115, 425-461.

Houze, R. A., (2004), Mesoscale convective systems. *Rev. Geophys*., 42, RG4003, doi:10.1029/2004RG000150.

Juracic, A., and D. J. Raymond, (2016), The effects of moist entropy and moisture budgets on tropical cyclone development. *J. Geophys. Res*., 121, 9458-9473.

Lindzen, R. S., and S. Nigam, (1987), On the role of sea surface temperature gradients in forcing low-level winds and convergence in the tropics, *J. Atmos. Sci.*, 44, 2418-2436.

Lopez Carrillo, C., and D. J. Raymond, (2011), Retrieval of three-dimensional wind fields from Doppler radar data using an efficient two-step approach. *Atmos. Meas. Tech.*, 4, 2717-2733, doi:10.5194/amt-4-2717-2011.

Montgomery, M. T., Davis, C., Dunkerton, T., Wang, Z., Velden, C., Torn, R., Majumdar, S. J., Zhang, F., Smith, R. K., Bosart, L., Bell, M. M., Haase, J. S., Heymsfield, A., Jensen, J., Campos, T., and Boothe, M. A., (2012), The Pre-Depression Investigation of Cloudsystems in the Tropics (PREDICT) experiment, *B. Am. Meteor. Soc*., 93, 153–172.

Palmen, E. H., (1948), On the Formation and Structure of Tropical Cyclones," *Geophysica, Helsinki*, Vol. 3, pp. 26-38.

Raymond, D. J., S. L. Sessions, and C. Lopez Carrillo, (2011), Thermodynamics of tropical cyclogenesis in the northwest Pacific, *J. Geophys. Res.*, 116, D18101, doi:10.1029/2011JD015624.

Raymond, D. J. and C. Lopez Carrillo, (2011), The vorticity budget of developing typhoon Nuri (2008), *Atmos. Chem. Phys.*, 11, 147-163, doi:10.5194/acp-11-147-2011.

Raymond, D. J., S. Gjorgjievska, S. Sessions, and Z. Fuchs, (2014), Tropical cyclogenesis and mid-level vorticity. *Australian Meteorological and Oceanographic Journal*, 64, 11-25.

Raymond, D. J., Z. Fuchs, S. Gjorgjievska and S. L. Sessions, (2015), Balanced dynamics and convection in the tropical troposphere. *J. Adv. Model. Earth Syst.*, 7, doi:10.1002/2015MS000467.

Raymond, D. J. and M. M. Flores, (2016), Predicting convective rainfall over tropical oceans from environmental conditions. *J. Adv. Model. Earth Syst.*, 8, doi:10.1002/2015MS000595.

Raymond, D. J., (2017), Convection in the east Pacific intertropical convergence zone. *Geophys. Res. Lett.*, 44, 562-568, doi:10.1002/2016GL071554.

Raymond, D. J. and G. Kilroy, (2019), Control of convection in high-resolution simulations of tropical cyclogenesis. *J. Adv. Model. Earth Syst.*, 11, 1582-1599.

Raymond and Fuchs-Stone, (2020), Emergent Properties of Convection in OTREC and PREDICT. *Journal of Geophysical Research: Atmospheres.*

Riehl, H., T. C. Yeh, J. S. Malkus and N. E, La Seur, (1951), The north-east trade of the Pacific ocean, *Quart. J. Roy. Meteor. Soc.*, 77, 598-626.

Sentić, S., Sessions, S. L., and Fuchs, Ž., (2015), Diagnosing DYNAMO convection with weak temperature gradient simulations, *J. Adv. Model. Earth Syst.*, 7, 1849– 1871, doi:10.1002/2015MS000531.

Sentić, S., Fuchs-Stone, Ž., & Raymond, D. J, (2020), The Madden-Julian Oscillation and mean easterly winds. *Journal of Geophysical Research: Atmospheres*, 125, e2019JD030869. https://doi.org/10.1029/2019JD030869

Singh, M. S., Warren, R. A., & Jakob, C., (2019), A steady-state model for the relationship between humidity, instability, and precipitation in the tropics. *Journal of Advances in Modeling Earth Systems*, **11**, 3973– 3994. https://doi.org/10.1029/2019MS001686

Stevens, B., J. Duan, J. C. McWilliams, M. Munnich, and J. D. Neelin, (2002), Entrainment, Rayleigh friction, and boundary layer winds over the tropical Pacific, *J. Climate*, 15, 30-44.

Tomas, R. A., J. R. Holton, and P. J. Webster, (1999), The influence of cross-equatorial pressure gradients on the location of near-equatorial convection, *Quart. J. Roy. Meteor. Soc.*, 125, 1107-1127.

UCAR/NCAR - Earth Observing Laboratory, Voemel, H. 2019. NCAR/EOL AVAPS Dropsonde QC Data. Version 1.0. UCAR/NCAR - Earth Observing Laboratory. https://doi.org/10.26023/EHRT-TN96-9W04. Accessed 13 January 2020.

Yu, L., Jin, X., & Weller, R. A, (2008), Multidecade global flux datasets from the Objectively Analyzed Air-sea Fluxes (OAFlux) Project: Latent and sensible heat fluxes, ocean evaporation, and related surface meteorological variables. Woods Hole Oceanographic Institution, OAFlux Project Technical Report. OA-2008-01, 64pp. Woods Hole, Massachusetts, USA.

Zipser, E. J., (1969), The role of organized unsaturated convective downdrafts in the structure and rapid decay of an equatorial disturbance. *J. Appl. Meteor.*, 8, 799-814.

Zipser, E. J., (1977), Mesoscale and convective scale downdrafts as distinct components of squall-line structure. *Mon. Wea. Rev.*, 105, 1568-1589.